Even-even Nd isotopes in an *SD*-pair shell model

B. C. He (何秉承) ⓘ, S. Y. Zhang (张思遥), Lei Li (李磊) ⓘ,* and Y. A. Luo (罗延安)†

School of Physics, Nankai University, Tianjin, 300071, People's Republic of China

Y. Zhang (张宇)

Department of Physics, Liaoning Normal University, Dalian 116029, People's Republic of China

F. Pan (潘峰)

Department of Physics, Liaoning Normal University, Dalian 116029, People's Republic of China
and Department of Physics and Astronomy, Louisiana State University, Baton Rouge, Louisiana 70803, USA

J. P. Draayer

Department of Physics and Astronomy, Louisiana State University, Baton Rouge, Louisiana 70803, USA

Nucleon pair shell model truncated to *SD* collective pair subspace (SDPSM) was applied to study the properties of the low-lying states of the even-even $^{144-156}$Nd isotopes. It is found that, within the M scheme, the systems with the number $N_\nu = 7$ of neutron pairs (or the number $N_\pi = 7$ of proton pairs) can be studied in the SDPSM for the first time. The results show that the properties of the low-lying states of the even-even Nd isotopes can be reproduced approximately, and the even-even $^{144-156}$Nd isotopes may be a good candidate for the first-order shape phase transition.

I. INTRODUCTION

In nuclear physics, the full-fledged shell model is a powerful microscopic method to describe nuclear structure. However, the huge number of configurations often surpasses the capability of the shell model. The nucleon pair shell model (NPSM) [1–4] was proposed in 1993, in which the building blocks of the configuration space are the nucleon pairs instead of the single valence nucleon. Guided by the success of the interacting boson model (IBM) [5] and interacting boson fermion model (IBFM) [6,7], one can truncate the full shell-model configuration space to a collective *S*-pair and *D*-pair subspace, which is called the *SD*-pair shell model (SDPSM) [8–10].

The SDPSM and its application have been studied extensively in the last two decades [11–19]. It was shown that the properties of the low-lying states of the even-even nuclei [13], the typical features of U(5), SU(3), and O(6) limiting cases, the shape evolution and the critical points properties in the IBM, can all be well reproduced in the SDPSM [20–22]. Therefore, the SDPSM can not only provide a sound shell-model foundation for the IBM but also demonstrate that the truncation scheme adopted in the SDPSM is reasonable [13].

Although the SDPSM can be used to reproduce the general behavior of the IBM, because the CPU time increases with

N_ν (N_π) dramatically, the systems studied in the SDPSM were still limited to the cases with $N_\pi(N_\nu) \leqslant 5$ [12].

In Ref. [23], the NPSM constructed in the M-scheme was proposed and it was found that the CPU time used in calculating the matrix elements can be reduced a lot. Moreover, Lei and his collaborators also found an efficient way to calculate the matrix elements in the M scheme [24]. These new techniques in the NPSM make it possible to study the well-deformed medium or heavy nuclei [23,24]. As an example, even-even $^{144-156}$Nd isotopes are studied in this paper.

The paper is organized as follows: In Sec. II we give a brief introduction of the model. The calculated results of the even-even Nd isotopes are discussed in Sec. III. And a brief summary and discussion are given in Sec. IV.

II. THE MODEL SCHEME

To study the properties of the even-even Nd isotopes, a Hamiltonian composed of the pairing plus quadrupole-quadrupole interactions is adopted, which is

$$\hat{H} = \sum_{\sigma=\pi,\nu} \hat{H}_\sigma - \kappa Q_\pi^2 \cdot Q_\nu^2,$$

$$\hat{H}_\sigma = H_{0\sigma} - G_{0\sigma} A^{(0)\dagger} \cdot A^{(0)} - G_{2\sigma} A^{(2)\dagger} \cdot A^{(2)\dagger} - \kappa_\sigma Q^2 \cdot Q^2,$$

$$H_{0\sigma} = \sum_a \epsilon_a C_a^\dagger C_a,$$

$$A^{(0)\dagger} = \sum_a \frac{\hat{a}}{2} (C_a^\dagger \times C_a^\dagger)^0,$$

*lilei@nankai.edu.cn
†luoya@nankai.edu.cn

$$A^{(2)\dagger} = \sum_{ab} q(ab2)(C_a^\dagger \times C_b^\dagger)^2,$$

$$\hat{a} = \sqrt{2j_a + 1}, \tag{1}$$

where $H_{0\sigma}$ is the single-particle (s.p.) energy term with $\sigma = \nu$ for neutrons and $\sigma = \pi$ for protons, G_0, G_2, and κ are the monopole pairing, quadrupole pairing, and quadrupole-quadrupole interactional strengths, respectively. $C_a^\dagger$ stands for the single-particle creation operator, where a denotes all possible quantum numbers (nlj) of the particle. $(C_a^\dagger \times C_b^\dagger)^t$ stands for two-particle coupled creation operator with total angular momentum t. The quadrupole operator $Q^{(2)}$ is defined as

$$Q_\mu^{(2)} = \sum_{cd} q(cd2)P_\mu^2(cd),$$

$$q(cd2) = (-1)^{j_c - \frac{1}{2}} \frac{\hat{j}_c \hat{j}_d}{\sqrt{20\pi}} C_{j_c \frac{1}{2}, j_d - \frac{1}{2}}^{20} \Delta_{cd2} \langle Nl_c | r^2 | Nl_d \rangle,$$

$$\Delta_{cd2} = \frac{1}{2}[1 + (-1)^{l_c + l_d + 2}],$$

$$P_\mu^2(cd) = (C_c^\dagger \times \tilde{C}_d)_\mu^2. \tag{2}$$

Here N is the principal quantum number of the spherical harmonic oscillator with energy $(N + \frac{3}{2})\hbar\omega_0$, l_c and l_d are the orbital angular-momentum quantum numbers of the single particle at levels c and d, respectively, $C_{j_c \frac{1}{2}, j_d - \frac{1}{2}}^{20}$ is the Clebsch-Gordan (CG) coefficient, and the time-reversal operator $\tilde{C}_a$ is defined as $\tilde{C}_{j_a m_a} = (-)^{j_a - m_a} C_{j_a - m_a}$. The matrix element $\langle Nl_c | r^2 | Nl_d \rangle$ is given by

$$\langle Nl_c | r^2 | Nl_d \rangle$$
$$= \begin{cases} (N + \frac{3}{2})r_0^2, & l_c = l_d \\ \varphi \sqrt{(N + l_d + 2 \pm 1)(N - l_d + 1 \mp 1)}\, r_0^2, & l_c = l_d \pm 2, \end{cases}$$

where the phase factor φ can be taken as ± 1, $r_0^2 = \frac{\hbar}{M_N \omega_0} = 1.012A^{\frac{1}{3}}$ fm^2, M_N is the mass of a nucleon, and ω_0 is the frequency of the harmonic oscillator. The $E2$ transition operator is simply taken as

$$T(E2) = e_\pi Q_\pi^{(2)} + e_\nu Q_\nu^{(2)}, \tag{3}$$

with e_σ ($\sigma = \pi, \nu$) being the effective charges for protons or neutrons.

The collective S pair and D pair are defined as

$$A_m^{r\dagger} = \sum_a y(abr)(C_a^\dagger \times C_b^\dagger)_m^r \quad (r = 0, 2), \tag{4}$$

where the structure coefficients satisfy the symmetry relation

$$y(abr) = -(-)^{j_a + j_b + r} y(bar). \tag{5}$$

As an approximation, the collective S-pair structure coefficients are chosen to be

$$y(aa0) = \hat{j}_a \frac{\nu_a}{\mu_a}, \tag{6}$$

where ν_a and μ_a are occupied and empty amplitudes obtained by solving the BCS equation, while the collective D-pair structure coefficients are obtained from the commutator,

$$A^{2\dagger} = D^\dagger = \tfrac{1}{2}[Q^2, S^\dagger]. \tag{7}$$

There are two schemes: the J scheme [3,8] and the M scheme [23,24], to constructed the multipair basis vector. In this work, the M scheme is adopted, which is defined as

$$|r_1 r_2 \cdots r_N; m_1, m_2 \cdots m_N, M\rangle$$
$$= A_{m_1}^{r_1} A_{m_2}^{r_2} \cdots A_{m_N}^{r_N} |0\rangle, \tag{8}$$

where r_i and m_i stand for the angular momentum and its projection of each collective pair, respectively. And the total projection M of the total angular momentum is given by

$$M = \sum_{i=1}^N m_i.$$

The overlap between two states is a key quantity, since the matrix elements of one-body and two-body interactions can all be expressed as a summation of the overlaps. The overlap between two states is

$$\langle 0|A_{M_1} A_{M_2}^\dagger |0\rangle \equiv \langle r_1\mu_1, \ldots r_N\mu_N; M_1 | s_1\nu_1, \ldots, s_N\nu_N; M_2\rangle$$

$$= \sum_{k=1}^N \Bigg[2\sum_{ab} y(abr_k)y(abs_N)\delta_{r_k,s_N}\delta_{\mu_k,\nu_N}$$

$$\times \langle r_1\mu_1 \cdots r_{k-1}\mu_{k-1}, r_{k+1}\mu_{k+1} \cdots r_N\mu_N; M_1 - \nu_N | s_1\nu_1 \cdots s_{N-1}\nu_{N-1}; M_2 - \nu_N\rangle + \sum_{i=k-1}^1 \sum_{r_i'\mu_i'}$$

$$\times \langle r_1\mu_1 \cdots r_i'\mu_i' \cdots r_{k-1}\mu_{k-1}, r_{k+1}\mu_{k+1} \cdots r_N\mu_N; M_1 - \nu_N | s_1\nu_1 \cdots s_{N-1}\nu_{N-1}; M_2 - \nu_N\rangle \Bigg], \tag{9}$$

where $r_i'\mu_i'$ is a new collective pair with

$$A_{-\mu_i'}^{r_i'} = \sum_{aa'} y'(aa'r_i')A_{-\mu_i'}^{r_i'}(aa'), \quad y'(aa'r_i') = z(aa'r_i') - (-)^{a+a'+r_i'}z(a'ar_i'),$$

$$z(aa'r_i') = -4\hat{r}_i\hat{r}_k\hat{s}\sum_{t\sigma}\hat{t}(-)^{r_k+r_i+r_i'-\mu_i}C_{r_i-\mu_i,t\sigma}^{r_i'\mu_i'}C_{r_k-\mu_k,s\mu}^{t\sigma}\sum_{bb'}y(a'b'r_i)y(abr_k)y(bb's)\begin{Bmatrix} r_k & s & t \\ a & b' & b \end{Bmatrix}\begin{Bmatrix} r_i & t & r_i' \\ a & a' & b' \end{Bmatrix}. \quad (10)$$

One can see that, although the overlap is still calculated recursively, the most time-consuming factor, the recoupling of the angular momentum, is not needed any more. The summation over the projection μ_i' of the new pair is redundant, since it is a constant value $\mu_i' = \mu_i + \mu_k - \nu_N$. The overlap for one pair state in M scheme is the same as that in the J-scheme, which is

$$\langle r_1\mu_1|s_1\nu_1\rangle = 2\delta_{r_1,s_1}\delta_{\mu_1,\nu_1}\sum_{ab}y(abr_1)y(abs_1). \quad (11)$$

More details of the model and its applications can be found in Refs. [3,8,10,24].

III. THE RESULTS

A. Parameters

To study the properties of the low-lying states of the even-even $^{144-156}$Nd, 50–82 ($0g_{7/2}$, $1d_{5/2}$, $1d_{3/2}$, $2s_{1/2}$, $0h_{11/2}$) and 82–126 ($1f_{7/2}$, $0h_{9/2}$, $1f_{5/2}$, $2p_{3/2}$, $2p_{1/2}$, $0i_{13/2}$) major shells coupled to the doubly closed nucleus ^{132}Sn are considered for protons and neutrons, respectively. The s.p. energies for neutrons and protons are fixed as the experimental data of ^{133}Sn and ^{133}Sb [25–27], and listed in Table I.

The parameters in Hamiltonian (1) are determined as follows: the monopole pairing interactional strengths are fixed as those used in Ref. [28], which are $G_{0\pi} = 0.14$, $G_{0\nu} = 0.12$ (in MeV) for protons and neutrons, respectively. The other parameters $G_{2\sigma}$, κ_σ, and κ are determined by fitting the low-lying spectra and listed in Table II.

B. Spectra

The low-lying spectra of the even-even Nd isotopes are presented in Fig. 1, from which one can see that the general agreement between the experiments and calculations is achieved for the low-lying states.

For ^{144}Nd, 2_1^+ and 4_1^+ states can be fit very well, but 6_1^+ and 8_1^+ states are higher than the experiments. Although 0_2^+, 2_2^+, 4_2^+, 2_3^+, and 3_1^+ states cannot be well fit in the SDPSM, except for the 0_2^+ state, which is lower than the 2_2^+ state, the

order of states, 2_2^+, 4_2^+, 2_3^+, and 3_1^+, is the same as that of the experiments.

For ^{146}Nd, 2_1^+, 4_1^+, and 6_1^+ states can be reproduced very well, but the calculated states with $J \geqslant 8$ are higher than the experiments. Although the calculated 0_2^+ and 2_2^+ states are lower than the experiments, the order of the two states is the same as that of the experiments; that is, the 0_2^+ state is lower than the 2_2^+ state.

For ^{148}Nd, 2_1^+, 4_1^+, and 6_1^+ states can be fit very well, and the states with $J \geqslant 8$ are higher than the experiments. Except for the 0_2^+ and 2_3^+ states, which are reproduced satisfactorily, the calculated 2_2^+ and 3_1^+ state are lower than the experiments, and the other states are higher than experiments.

For ^{150}Nd, 2_1^+, 4_1^+, and 6_1^+ states can be fit approximately. The states with $J \geqslant 8$ are still higher than the experiments. Except for the 3_1^+ and 2_3^+ states, the other states, 0_2^+, 2_2^+, 2_3^+, 4_2^+, 5_1^+, and 6_2^+ states are all close to the experimental values.

For $^{152-156}$Nd, 2_1^+, 4_1^+, and 6_1^+ states can be reproduced very well, and the states with $J \geqslant 8$ are also higher than the experiments.

It is known that only the S and D collective pairs are included in the SDPSM. The fact that the states with $J \geqslant 8$ cannot be reproduced satisfactorily in the SDPSM may imply that the truncation of the shell-model space to collective S-pair and D-pair subspace is a good approximation for the low-lying states, while it is too small for the high-lying states.

From Fig. 1, one can also see that, although the calculated 6_1^+ and 8_1^+ states are higher than the experiments for the even-even Nd isotopes, the larger the number of the neutron pairs, the better the agreement between the calculations and experiments.

It is known that the evolution of nuclear structure (shape) with N_ν (N_π) often exhibit quantum phase transitions (QPTs), or called shape phase transitions (SPTs). Lots of related issues have been studied [29–48] since the two analytical descriptions of critical-point symmetry known as X(5) and E(5) for first- and second-order spherical-deformed phase transitions [49,50], respectively, were introduced in the collective model

TABLE I. Adopted s.p. energies ϵ_σ ($\sigma = \pi$ *or* ν) for protons (50–82 shell) and neutrons (82–126 shell) (in units of MeV).

j_ν	$1f_{7/2}$	$0h_{9/2}$	$1f_{5/2}$	$2p_{3/2}$	$2p_{1/2}$	$0i_{13/2}$
ϵ_ν	0	1.561	2.005	0.854	1.656	1.8

j_π	$0g_{7/2}$	$1d_{5/2}$	$1d_{3/2}$	$2s_{1/2}$	$0h_{11/2}$
ϵ_π	0	0.963	2.69	2.99	2.76

TABLE II. The parameters (in units of MeV/r_0^4) used for each nucleus.

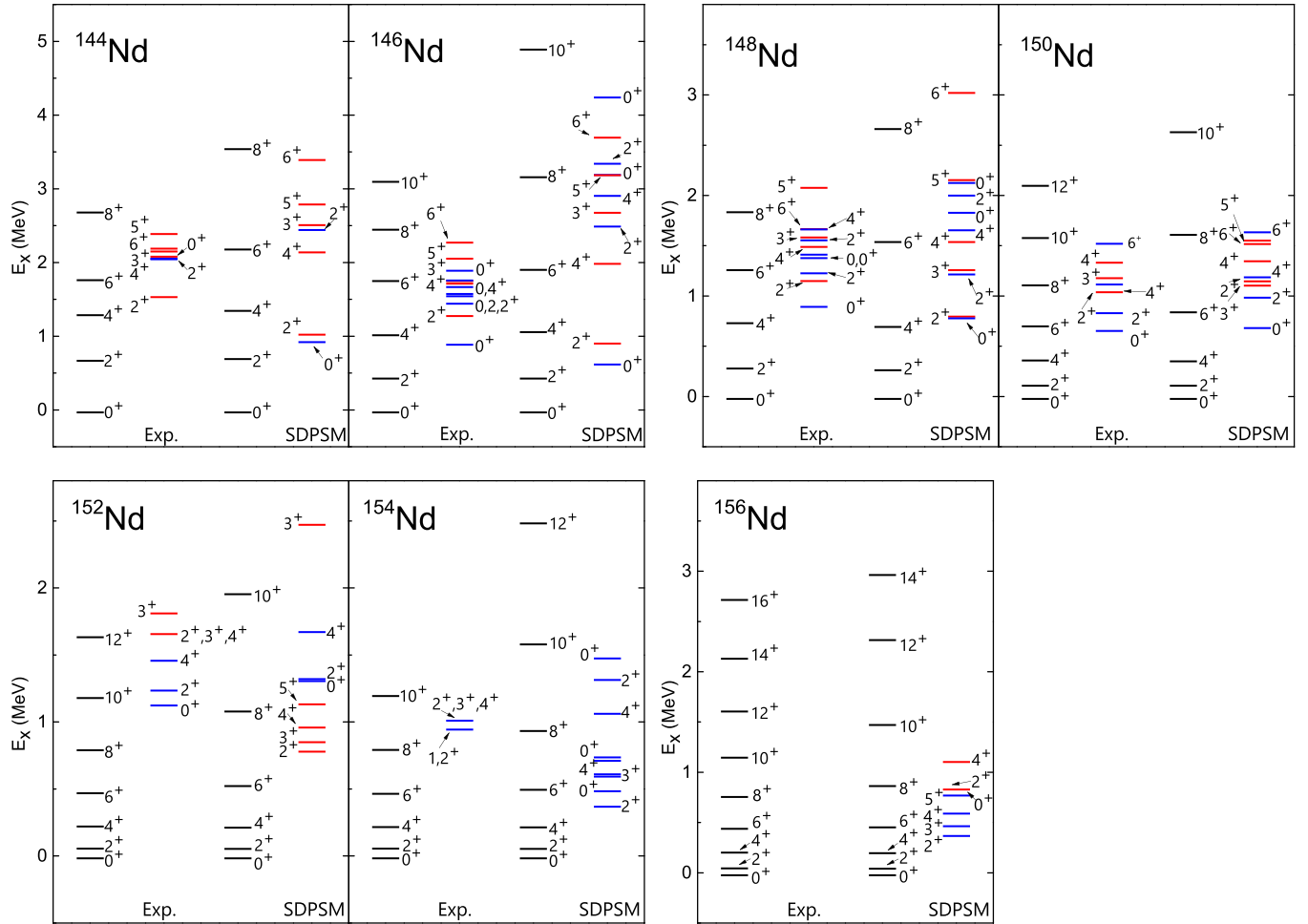|	^{144}Nd	^{146}Nd	^{148}Nd	^{150}Nd	^{152}Nd	^{154}Nd	^{156}Nd
$G_{2\pi}$	0.054	0.045	0.028	0.022	−0.01	0.015	0.015
$G_{2\nu}$	0.039	0.015	0.025	0.030	0.033	0.032	0.035
$\kappa_{2\pi}$	0.008	−0.012	−0.038	0.011	−0.100	0.023	0.012
$\kappa_{2\nu}$	0.030	0.010	−0.023	0.030	0.011	−0.010	−0.010
κ	0.260	0.192	0.175	0.100	0.110	0.150	0.176

FIG. 1. The low-lying energy spectra of Nd isotopes. The experimental data are taken from Ref. [25].

[51]. It is known that the even-even $^{144-152}$Nd isotopes may be a realistic case of the first-order QPTs. Therefore, it is interesting to study if the behavior of the QPTs can be reproduced in the SDPSM. To this end, some widely used effective parameters [52–56], the energy ratios $R_{42} = E_{4_1^+}/E_{2_1^+}$, $R_{02} = E_{0_2^+}/E_{2_1^+}$, and $R_{60} = E_{6_1^+}/E_{0_1^+}$, are studied with the results given in Figs. 2–4.

From Fig. 2 one can see that the experimental results can be reproduced very well. The predicted R_{42} for ^{150}Nd is 2.87, close to the experimental value 2.93 and the value of X(5) symmetry 2.91 [57]. The calculated results for ^{152}Nd, ^{154}Nd, and ^{156}Nd are 3.26, 3.27, and 3.32, respectively, which are close to the experimental results reaching nearly the rotational limit 3.33. The overall trend of R_{42} for Nd isotopes can be well reproduced. Figure 3 shows that, except for ^{144}Nd, for which the calculated result is smaller than the experimental value, R_{02} increases with N_ν, and the general trend of R_{02} can be well reproduced in the SDPSM. For R_{60}, as shown in Fig. 4, the variation trends of the experiments and calculations are similar, the maximal values occur around ^{146}Nd, and then they decrease with N_ν. Since the predicted 0_2^+ states for ^{144}Nd and ^{146}Nd are lower than those of the experiments, the calculated R_{60} are larger than the experimental values. The calculated
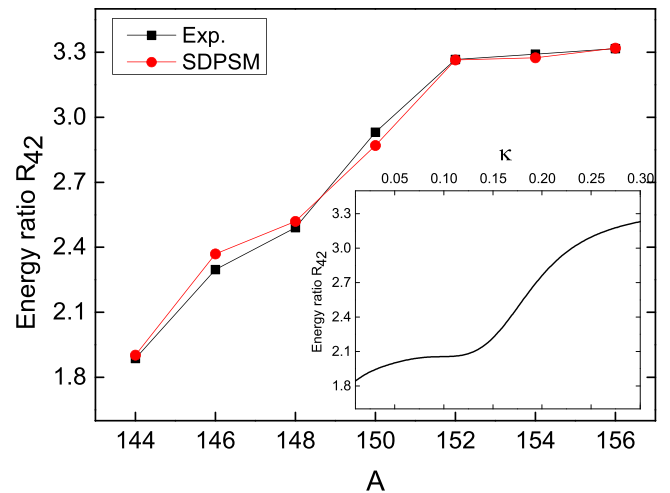

FIG. 2. The experimental and calculated energy ratio R_{42} of even-even $^{144-156}$Nd isotopes. The experimental data are taken from Ref. [25]. R_{42} vs κ for the system with $N_\pi = 5$ and $N_\nu = 3$ is shown in the inset, where the parameters are fixed as $G_{0\pi} = 0.14$ MeV, $G_{0\nu} = 0.12$ MeV, $G_{2\pi} = G_{2\nu} = 0$, $\kappa_\pi = \kappa_\nu = 0$, and κ changes from 0 to 0.3 MeV/r_0^4.
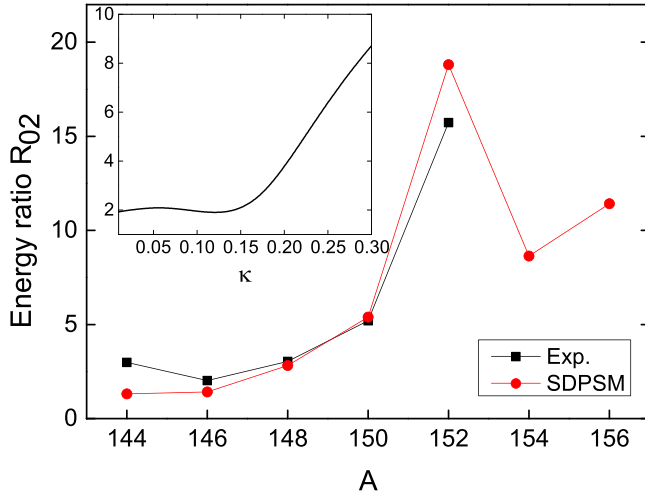
FIG. 3. The experimental and calculated energy ratio R_{02} of even-even $^{144-156}$Nd isotopes. The experimental data are taken from Ref. [25]. R_{02} vs κ for the system with $N_\pi = 5$ and $N_\nu = 3$ is shown in the inset, where the parameters are fixed as $G_{0\pi} = 0.14$ MeV, $G_{0\nu} = 0.12$ MeV, $G_{2\pi} = G_{2\nu} = 0$, $\kappa_\pi = \kappa_\nu = 0$, and κ changes from 0 to 0.3 MeV/r_0^4.

R_{02} and R_{60} for ^{154}Nd and ^{156}Nd are also provided, but no experimental values are available.

Our previous works [21,22] show that the typical QPTs features given in the IBM can be reproduced in the SDPSM, i.e., some widely used effective parameters studied in the IBM can be reproduced by changing the control parameters (or the interactional strengths). To reveal if the general behavior of the QPTs from spherical to rotational pattern can be reproduced in the SDPSM for the even-even Nd isotopes, the energy ratios R_{42}, R_{02}, and R_{60} changing with the proton-
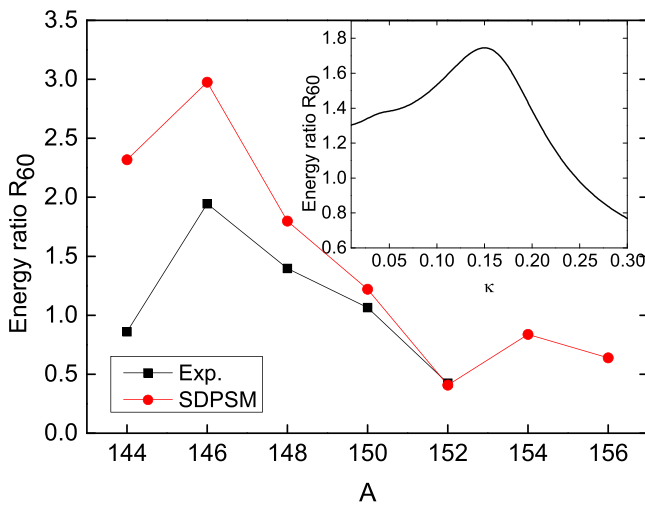

FIG. 4. The experimental and calculated energy ratio R_{60} of even-even $^{144-156}$Nd isotopes. The experimental data are taken from Ref. [25]. R_{60} vs κ for the system with $N_\pi = 5$ and $N_\nu = 3$ is shown in the inset, where the parameters are fixed as $G_{0\pi} = 0.14$ MeV, $G_{0\nu} = 0.12$ MeV, $G_{2\pi} = G_{2\nu} = 0$, $\kappa_\pi = \kappa_\nu = 0$, and κ changes from 0 to 0.3 MeV/r_0^4.

neutron quadrupole interaction strength are presented for the system with $N_\pi = 5$ and $N_\nu = 3$. The parameters we used are $G_{0\pi} = 0.14$ MeV, $G_{0\nu} = 0.12$ MeV, $G_{2\pi} = G_{2\nu} = 0$, $\kappa_\pi = \kappa_\nu = 0$, and κ changes from 0 to 0.3 MeV/r_0^4. The calculated results are inserted in Figs. 2–4. From the inserted figures, one can clearly see that the general behavior of the QPTs from spherical to rotational pattern can be exhibited in the evolutions the even-even Nd isotopes.

C. *B(E2)* values

To further study if the SDPSM can reproduce the properties of the low-lying states of the even-even Nd isotopes, $B(E2)$ values are taken to be compared between the theoretical calculations and the experiments. By fitting $B(E2; 0_1^+ \to 2_1^+)$ of ^{144}Nd, the effective charges in Eq. (3) are fixed as $e_\pi = 2.0e$ for protons and $e_\nu = 1.0e$ for neutrons, which are close to the values adopted in the other works in the SDPSM [28,58].

Calculated $B(E2)$ values and the available experimental data are listed in Table III, from which one can see that for $B(E2; 0_1^+ \to 2_1^+)$, the calculated results are close to the experimental data for ^{144}Nd and ^{146}Nd. From ^{148}Nd on, the difference between the experiments and the calculations increases with N_ν. For example, the experimental value for ^{148}Nd is 1.37(2) $(eb)^2$, while the SDPSM result is 0.912 $(eb)^2$, and for ^{152}Nd the experimental value and calculated result are 4.20(28) $(eb)^2$ and 1.850 $(eb)^2$, respectively. Table III also shows that the calculated results of $B(E2; 0_1^+ \to 2_2^+)$ are close to those of the available experimental data.

It is known that $B(E2; 2_1^+ \to 0_1^+) = \frac{1}{5} B(E2; 0_1^+ \to 2_1^+)$, since some available experimental data for $B(E2; 2_1^+ \to 0_1^+)$ are inconsistent with $\frac{1}{5} B(E2; 0_1^+ \to 2_1^+)$ within the errors, $B(E2; 2_1^+ \to 0_1^+)$ are also listed in Table III. It is seen that, for ^{144}Nd, the experimental value of $B(E2; 2_1^+ \to 0_1^+)$ is smaller than $\frac{1}{5} B(E2; 0_1^+ \to 2_1^+)$ and also smaller than the calculated value. For the other nuclei, $B(E2; 2_1^+ \to 0_1^+)$ is about $\frac{1}{5} B(E2; 0_1^+ \to 2_1^+)$ for both experiments and the calculations, and the calculated results are all smaller than those of the experimental data. For $B(E2; 4_1^+ \to 2_1^+)$, except for ^{146}Nd, for which the calculated result is larger than that of the experimental value, they are about half of the experimental values. Especially for ^{150}Nd, the experimental data are 0.857(8) $(eb)^2$, while the SDPSM result is 0.412 $(eb)^2$. For $B(E2; 0_2^+ \to 2_1^+)$, two experimental data are available, but only one can be well reproduced. Specially, the experimental data are 0.145(10) $(eb)^2$ and 0.204(11) $(eb)^2$ for ^{148}Nd and ^{150}Nd, respectively, and the calculated results for the two nuclei are 0.152 $(eb)^2$ and 0.104 $(eb)^2$. For $B(E2; 2_2^+ \to 2_1^+)$, one can see that the SDPSM results are all smaller than the experimental data, and the larger the number of the neutron pairs, the smaller the relative difference. For example, $\frac{B(E2; 2_2^+ \to 2_1^+)_{\text{expt}} - B(E2; 2_2^+ \to 2_1^+)_{\text{theor}}}{B(E2; 2_2^+ \to 2_1^+)_{\text{expt}}} = 0.98$ is given for ^{144}Nd, while it is 0.6 for ^{150}Nd.

To study the $E2$ transition further, the relative $B(E2)$ ratios are also studied with the results listed in Table IV. It is seen that for $\frac{B(E2; 4_1^+ \to 2_1^+)}{B(E2; 2_1^+ \to 0_1^+)}$, except for ^{144}Nd, which is smaller than the experimental value, the calculated results are close to the experimental data. For $\frac{B(E2; 0_1^+ \to 2_1^+)}{B(E2; 2_1^+ \to 0_1^+)}$, $\frac{B(E2; 0_2^+ \to 2_1^+)}{B(E2; 2_1^+ \to 0_1^+)}$, and

TABLE III. The $B(E2)$ values (in $(eb)^2$) of $^{144-156}$Nd.

| | ^{144}Nd | | ^{146}Nd | | ^{148}Nd | | ^{150}Nd | | ^{152}Nd | | ^{154}Nd | | ^{156}Nd | |
	Expt.	Theor.	Expt.	Theor.	Expt.	Theor.	Expt.	Theor.	Expt.	Theor.	Expt.	Theor.	Expt.	Theor.
$B(E2; 0^+_1 \rightarrow 2^+_1)$[a]	0.491(5)	0.489	0.760(23)	0.758	1.37(2)[b]	0.912	2.72(2)[b]	1.447	4.20(28)	1.850		1.976		2.209
$B(E2; 0^+_1 \rightarrow 2^+_2)$	0.0030(4)[c]	0.022	0.073(2)[c]	0.055	0.020(2)[b]	0.036	0.012(1)[b]	0.016		0.004		0.006		0.005
$B(E2; 2^+_1 \rightarrow 0^+_1)$	0.076(4)[d]	0.098	0.146(1)[e]	0.152	0.270(10)[f]	0.182	0.550(14)[g]	0.289	0.835(48)[h]	0.370	0.466(123)[j]	0.395		0.442
$B(E2; 4^+_1 \rightarrow 2^+_1)$[j]	0.084(10)[d]	0.032	0.197(50)[e]	0.226	0.438(19)[f]	0.268	0.857(8)[g]	0.412	1.091(53)[h]	0.523		0.579		0.639
$B(E2; 0^+_2 \rightarrow 2^+_1)$		0.043		0.239	0.145(10)[f]	0.152	0.204(11)[g]	0.104		0.024		0.003		0.002
$B(E2; 2^+_2 \rightarrow 2^+_1)$[j]	0.095(40)	0.002	0.090(6)	0.008	0.12(1)	0.045	0.035(5)	0.014		0.001		0.002		0.001

[a]Ref. [59].
[b]Ref. [25].
[c]Ref. [60].
[d]Ref. [61].
[e]Ref. [62].
[f]Ref. [63].
[g]Ref. [64].
[h]Ref. [65].
[i]Ref. [66].
[j]Ref. [67].

TABLE IV. The relative $B(E2)$ values of $^{144-156}$Nd.

	^{144}Nd		^{146}Nd		^{148}Nd		^{150}Nd		^{152}Nd		^{154}Nd		^{156}Nd	
	Expt.	Theor.	Expt.	Theor.	Expt.	Theor.	Expt.	Theor.	Expt.	Theor.	Expt.	Theor.	Expt.	Theor.
$\frac{B(E2;4^+_1\to 2^+_1)}{B(E2;2^+_1\to 0^+_1)}$	1.11	0.33	1.35	1.48	1.62	1.47	1.56	1.42	1.31	1.41		1.47		1.45
$\frac{B(E2;0^+_2\to 2^+_1)}{B(E2;2^+_1\to 0^+_1)}$	6.46	4.99	5.21	4.99	5.07	5.01	4.95	5.01	5.03	5.00		5.00		5.00
$\frac{B(E2;0^+_3\to 2^+_1)}{B(E2;2^+_1\to 0^+_1)}$		0.43		1.57	0.54	0.84	0.37	0.36		0.06		0.01		0
$\frac{B(E2;2^+_2\to 2^+_1)}{B(E2;2^+_1\to 0^+_1)}$	1.25	0.02	0.62	0.05	0.44	0.25	0.06	0.05		0		0.01		0
$\frac{B(E2;0^+_1\to 2^+_2)}{B(E2;2^+_1\to 0^+_1)}$	0.04	0.74	0.50	0.36	0.07	0.20	0.02	0.06		0.01		0.02		0.01

$\frac{B(E2;0^+_1\to 2^+_2)}{B(E2;2^+_1\to 0^+_1)}$, the available experimental data can be reproduced approximately. For example, the available experimental value of $\frac{B(E2;0^+_1\to 2^+_1)}{B(E2;2^+_1\to 0^+_1)}$ is 5.07 for ^{148}Nd, and the calculated value is 5.01. The calculated $\frac{B(E2;2^+_2\to 2^+_1)}{B(E2;2^+_1\to 0^+_1)}$ are much smaller than the experiments for ^{144}Nd and ^{146}Nd. The results for the other nuclei are reasonable. From above analysis one can see that the experimental $B(E2)$ ratios can be reproduced approximately for even-even Nd isotopes.

It is known that in addition to the energy ratios, $B(E2)$ ratios $K_1 = B(E2;4^+_1 \to 2^+_1)/B(E2;2^+_1 \to 0^+_1)$ and $K_2 = B(E2;0^+_2 \to 2^+_1)/B(E2;2^+_1 \to 0^+_1)$ [55] can also be used to characterize the QPTs. Therefore, to study the QPTs of the Nd isotopes in the SDPSM, K_1 and K_2 are shown in Fig. 5. It is seen that, although K_1 for ^{144}Nd is smaller than the experiment, the general behavior of K_1 can be reproduced in the SDPSM, i.e., both the calculated results and the experimental data increase with N_ν first, and then decrease with N_ν. There are only two available experimental data for K_2. From Fig. 5 one can see that, although the calculated results for the two nuclei are smaller than the experimental values, their evolutional behavior of ν is similar to that of the experiments: both of them decrease with N_ν.

To see the QPTs clearly, as in Sec. III B, K_1 and K_2 against κ are also studied for the system with $N_\pi = 5$ and $N_\nu = 3$. The parameters are still fixed as $G_{0\pi} = 0.14$ MeV, $G_{0\nu} = 0.12$ MeV, $G_{2\pi} = G_{2\nu} = 0$, $\kappa_\pi = \kappa_\nu = 0$, and κ changes from 0 to 0.3 MeV/r_0^4. The calculated results are inserted in Fig. 5. One can clearly see that K_1 and K_2 are consistent with our previous study of the first-order QPTs in the SDPSM [22] and the IBM [43], and the general behavior of K_1 and K_2 against κ are similar to the results calculated for the even-even Nd isotopes. Namely, the QPTs from spherical to rotational pattern can be approximately reproduced, indicating that the even-even $^{144-156}$Nd isotopes may be a good candidate for the first-order QPTs.

IV. SUMMARY AND DISCUSSION

In this work, the even-even $^{144-156}$Nd isotopes have been studied in the SDPSM. By studying the spectra and $E2$ transitions between some low-lying states, it was found that the properties of the low-lying states for the even-even Nd isotopes can be reproduced approximately. The QPTs from spherical to rotational pattern can also be reproduced approximately, which may imply that the even-even $^{144-156}$Nd isotopes may be a good candidate for the first order QPTs.
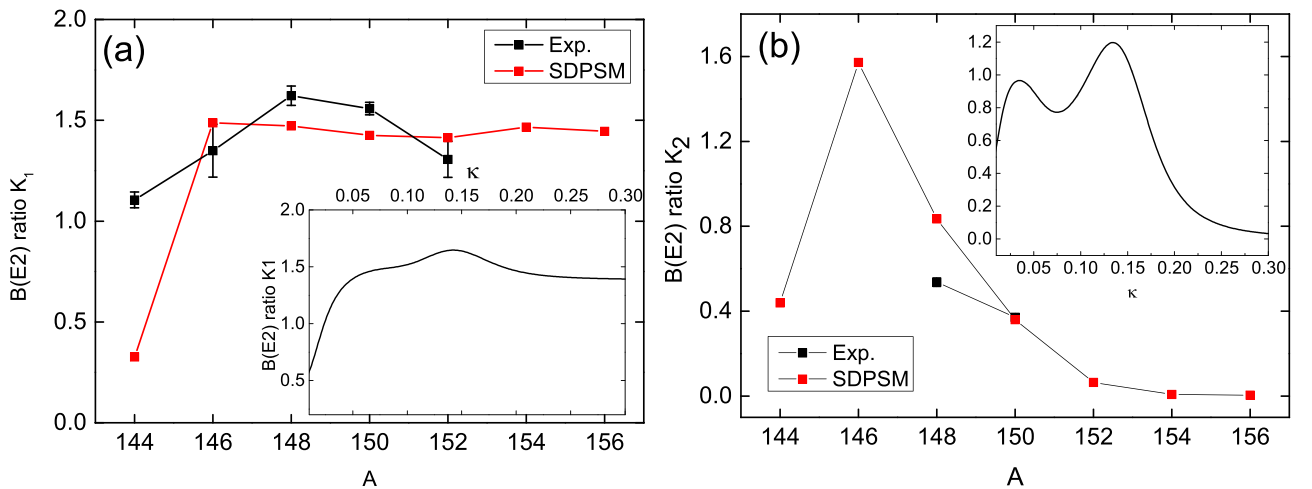

FIG. 5. The experimental and calculated $B(E2)$ ratios K_1 and K_2 of even-even $^{144-156}$Nd isotopes are shown in panels (a) and (b), respectively. K_1 and K_2 vs κ for the system with $N_\pi = 5$ and $N_\nu = 3$ are shown in the inset, where the parameters are fixed as $G_{0\pi} = 0.14$ MeV, $G_{0\nu} = 0.12$ MeV, $G_{2\pi} = G_{2\nu} = 0$, $\kappa_\pi = \kappa_\nu = 0$, and κ changes from 0 to 0.3 MeV/r_0^4.

It is known that the effective residual interactions increase with the number of valence nucleons linearly or quadratically for the short- and long-range forces, respectively, one expects that the S-pair and D-pair truncation is better for the system with larger number of valence particles or holes in reproducing the collectivity of the low-lying states. From above analysis one can notice that for the spectra, the larger the number of the valence nucleon-pairs, the better the agreement between experiments and calculations. Although the calculated $B(E2)$ values increase with N_ν, they are not as strong as those of the experiments. The larger the number of the valence neutrons, the larger the difference between the experiments and calculations. The effect of the s.p. energies is opposite to those of the residual interactions. In our calculation, the s.p. energies are fixed for all the Nd isotopes. The s.p. energy levels may depend on the number of valence nucleons. From the IBM microscopic calculation [68], it was found that, in order to account for the properties of Te, Xe, and Ba isotopes, the s.p. energies should be taken as more compressed as number of valence nucleons or holes increases. As we know that the s.p. energy term has important influence on the nuclear collectivity [11], a compressing of the s.p. spectrum maybe enhance the collectivity considerably and thus improve the behavior of the $B(E2)$ value versus the number of the valence nucleons. What is more, the model space is limited to 50–82 and 82–126 major shells for protons and neutrons, respectively, because of the limited model space, the Pauli blocking effect increases with N_ν, and thus the collectivity of low-lying states decreases with N_ν.

In summary, due to the CPU time in calculating the matrix elements increases with N_ν dramatically, our previous work in the SDPSM was limited to the cases with $N_\nu \leqslant 5$ and $(N_\pi) < 5$ [12], whereas this time we study the systems with $N_\nu \geqslant 5$ and $(N_\pi \geqslant 5)$ in the SDPSM. The results indicate that the SDPSM can reproduce the properties of low-lying states of the even-even Nd isotopes, which in turn suggests that it is possible to use the SDPSM to describe the properties of low-lying states of nuclei from closed-shell to neutron-rich nuclei. More work of the validity of the SDPSM for well-deformed nuclei and QPTs will be reported elsewhere.

[1] J.-Q. Chen, Nucl. Phys. A **562**, 218 (1993).
[2] J.-Q. Chen, B.-Q. Chen, and A. Klein, Nucl. Phys. A **554**, 61 (1993).
[3] J. Q. Chen, Nucl. Phys. A **626**, 686 (1997).
[4] J.-Q. Chen and Y.-A. Luo, Nucl. Phys. A **639**, 615 (1998).
[5] F. Iachello and A. Arima, *The Interacting Boson Model (Cambridge Monographs on Mathematical Physics)* (Cambridge University Press, Cambridge, 1987).
[6] F. Iachello and I. P. Van, *The Interacting Boson-Fermion Model* (Cambridge University Press, 1991).
[7] A. Arima and F. Iachello, Phys. Rev. C **14**, 761 (1976).
[8] Y. Zhao and A. Arima, Phys. Rep. **545**, 1 (2014).
[9] Y. M. Zhao, N. Yoshinaga, S. Yamaji, J. Q. Chen, and A. Arima, Phys. Rev. C **62**, 014304 (2000).
[10] Y.-A. Luo, J.-Q. Chen, and J. Draayer, Nucl. Phys. A **669**, 101 (2000).
[11] L. Yan-An and J.-Q. Chen, Phys. Rev. C **58**, 589 (1998).
[12] X.-f. Meng, F.-r. Wang, Y.-a. Luo, F. Pan, and J. P. Draayer, Phys. Rev. C **77**, 047304 (2008).
[13] Y.-A. Luo, F. Pan, C. Bahri, and J. P. Draayer, Phys. Rev. C **71**, 044304 (2005).
[14] Y. Y. Cheng, Y. Lei, Y. M. Zhao, and A. Arima, Phys. Rev. C **92**, 064320 (2015).
[15] Y. M. Zhao, S. Pittel, R. Bijker, A. Frank, and A. Arima, Phys. Rev. C **66**, 041301(R) (2002).
[16] K. Higashiyama, N. Yoshinaga, and K. Tanabe, Phys. Rev. C **65**, 054317 (2002).

[17] G. J. Fu, Y. Lei, Y. M. Zhao, S. Pittel, and A. Arima, Phys. Rev. C **87**, 044310 (2013).
[18] Y. Y. Cheng, Y. M. Zhao, and A. Arima, Phys. Rev. C **97**, 024303 (2018).
[19] Y. Bao, Y. Y. Cheng, and X.-R. Zhou, Phys. Rev. C **104**, 034312 (2021).
[20] Y. A. Luo, F. Pan, P. Z. Ning, and J. P. Draayer, Chin. Phys. Lett. **22**, 1366 (2005).
[21] Y.-A. Luo, F. Pan, T. Wang, P.-Z. Ning, and J. P. Draayer, Phys. Rev. C **73**, 044323 (2006).
[22] Y. Luo, Y. Zhang, X. Meng, F. Pan, and J. P. Draayer, Phys. Rev. C **80**, 014311 (2009).
[23] B. C. He, L. Li, Y. A. Luo, Y. Zhang, F. Pan, and J. P. Draayer, Phys. Rev. C **102**, 024304 (2020).
[24] Y. Lei, Y. Lu, and Y. M. Zhao, Chinese Phys. C **45**, 054103 (2021).
[25] National Nuclear Data Center, Brookhaven National Laboratory.
[26] F. Andreozzi, L. Coraggio, A. Covello, A. Gargano, T. T. S. Kuo, and A. Porrino, Phys. Rev. C **56**, R16 (1997).
[27] W. Urban, W. Kurcewicz, A. Nowak, T. Rząca-Urban, J. L. Durell, M. J. Leddy, M. A. Jones, W. R. Phillips, A. G. Smith, and B. J. Varley, Eur. Phys. J. A **5**, 239 (1999).
[28] L. Y. Jia, H. Zhang, and Y. M. Zhao, Phys. Rev. C **75**, 034307 (2007).
[29] R. F. Casten, J. Phys. G: Nucl. Part. Phys. **62**, 183 (2009).
[30] P. Cejnar and J. Jolie, Prog. Part. Nucl. Phys. **62**, 210 (2009).
[31] M. Caprio, P. Cejnar, and F. Iachello, Ann. Phys. (NY) **323**, 1106 (2008).

[32] P. Cejnar, J. Jolie, and R. F. Casten, Rev. Mod. Phys. **82**, 2155 (2010).

[33] A. Arima and F. Iachello, Ann. Phys. (NY) **99**, 253 (1976).

[34] A. Arima and F. Iachello, Ann. Phys. (NY) **111**, 201 (1978).

[35] A. Arima and F. Iachello, Ann. Phys. (NY) **123**, 468 (1979).

[36] K. Kaneko, M. Hasegawa, and T. Mizusaki, Phys. Rev. C **70**, 051301(R) (2004).

[37] M. Hasegawa, K. Kaneko, T. Mizusaki, and Y. Sun, Phys. Lett. B **656**, 51 (2007).

[38] N. Mărginean, S. Lenzi, A. Gadea, E. Farnea, S. Freeman, D. Napoli, D. Bazzacco, S. Beghini, B. Behera, P. Bizzeti, *et al.*, Phys. Lett. B **633**, 696 (2006).

[39] Y. Sun, P. M. Walker, F.-R. Xu, and Y.-X. Liu, Phys. Lett. B **659**, 165 (2008).

[40] N. Shimizu, T. Otsuka, T. Mizusaki, and M. Honma, Phys. Rev. Lett. **86**, 1171 (2001).

[41] T. Otsuka, M. Honma, T. Mizusaki, N. Shimizu, and Y. Utsuno, Prog. Part. Nucl. Phys. **47**, 319 (2001).

[42] N. Shimizu, T. Otsuka, T. Mizusaki, and M. Honma, Phys. Rev. C **70**, 054313 (2004).

[43] Z. feng Hou, Y. Zhang, and Y. xin Liu, Phys. Lett. B **688**, 298 (2010).

[44] D. Bonatsos, I. E. Assimakis, N. Minkov, A. Martinou, S. Sarantopoulou, R. B. Cakirli, R. F. Casten, and K. Blaum, Phys. Rev. C **95**, 064326 (2017).

[45] B. Li, F. Pan, and J. P. Draayer, Phys. Rev. C **93**, 044312 (2016).

[46] T. Nikšić, D. Vretenar, G. A. Lalazissis, and P. Ring, Phys. Rev. Lett. **99**, 092502 (2007).

[47] J. Meng, W. Zhang, S. G. Zhou, H. Toki, and L. S. Geng, Eur. Phys. J. A **25**, 23 (2005).

[48] Z. P. Li, T. Nikšić, D. Vretenar, and J. Meng, Phys. Rev. C **80**, 061301(R) (2009).

[49] F. Iachello, Phys. Rev. Lett. **85**, 3580 (2000).

[50] F. Iachello, Phys. Rev. Lett. **87**, 052502 (2001).

[51] A. N. Bohr and B. R. Mottelson, Collective and individual-particle aspects of nuclear structure. Dan. Mat. Fys. Medd., **27**(CERN-57-38), 1 (1953).

[52] F. Pan, J. P. Draayer, and Y. Luo, Phys. Lett. B **576**, 297 (2003).

[53] D. J. Rowe, P. S. Turner, and G. Rosensteel, Phys. Rev. Lett. **93**, 232502 (2004).

[54] F. Iachello and N. V. Zamfir, Phys. Rev. Lett. **92**, 212501 (2004).

[55] Y. Zhang, Z.-f. Hou, and Y.-x. Liu, Phys. Rev. C **76**, 011305(R) (2007).

[56] D. Bonatsos, E. A. McCutchan, R. F. Casten, and R. J. Casperson, Phys. Rev. Lett. **100**, 142501 (2008).

[57] R. Krücken, B. Albanna, C. Bialik, R. F. Casten, J. R. Cooper, A. Dewald, N. V. Zamfir, C. J. Barton, C. W. Beausang, M. A. Caprio, *et al.*, Phys. Rev. Lett. **88**, 232501 (2002).

[58] L. Y. Jia, H. Zhang, and Y. M. Zhao, Phys. Rev. C **76**, 054305 (2007).

[59] S. Raman, C. W. N. Jr., and P. Tikkanen, At. Data Nucl. Data Tables **78**, 1 (2001).

[60] J. B. Gupta, Phys. Rev. C **92**, 044316 (2015).

[61] J. Tuli, Nucl. Data Sheets **56**, 607 (1989).

[62] Y. Khazov, A. Rodionov, and G. Shulyak, Nucl. Data Sheets **136**, 163 (2016).

[63] N. Nica, Nucl. Data Sheets **117**, 1 (2014).

[64] S. Basu and A. Sonzogni, Nucl. Data Sheets **114**, 435 (2013).

[65] M. Martin, Nucl. Data Sheets **114**, 1497 (2013).

[66] C. Reich, Nucl. Data Sheets **110**, 2257 (2009).

[67] J. B. Gupta, J. Phys. G **21**, 565 (1995).

[68] T. Mizusaki and T. Otsuka, Prog. Theor. Phys. Suppl. **125**, 97 (1996).